Sonic Hedgehog is not a limb morphogen but acts as a trigger to specify all digits

Jianjian Zhu[1], Anna Trofka[1], Brian D. Harfe[2], Susan Mackem[1*]

[1]Cancer and Developmental Biology Laboratory, Center for Cancer Research, NCI, Frederick, MD

[2] College of Medicine, Dept of Molecular Genetics and Microbiology and the Genetics Institute, University of Florida, Gainesville, FL

*author for correspondence: mackems@mail.nih.gov

Summary

Limb patterning by Sonic hedgehog (Shh) is among the most highly touted and studied models of "morphogen" function[1]. Yet how Shh instructs distinct digit types (index to little finger) remains controversial. Both spatial concentration gradients[2,3] and temporal signal integration[4-6] have been proposed to explain how Shh patterns different digits, yet genetic studies in mouse suggested that Shh acts over a limited interval to specify digits[7]. Here, we replaced the cell survival function of Shh during limb bud outgrowth and demonstrate that a transient, early pulse of Shh activity is necessary and sufficient for normal limb development. Our lineage tracing of Shh response shows that Shh signals at very short-range during this time frame and patterns digits indirectly. We demonstrate that Gli3, the major Shh nuclear transducer[8,9], is functionally unaltered and cryptic pathway re-activation doesn't occur. Our findings are incompatible with either spatial or temporal signal integration models and indicate Shh initiates a relay mechanism. Using a genetic test for relay signaling, we unexpectedly discovered that Shh is required indirectly to specify digit 1 (thumb), previously thought to be exclusively Shh-independent[10,11]. Our results uncover a unique digit 1 regulatory hierarchy, implicating Shh in digit 1 evolutionary adaptations, such as an opposable thumb. These findings illuminate Shh function in the related contexts of limb development, regeneration, and evolutionary adaptation, and lay the groundwork for elucidating how Shh triggers a relay network that becomes rapidly self-sustaining.

Introduction

The limb and neural tube have been mainstays for elucidating vertebrate Hedgehog morphogen function. In contrast to neural tube, anterior-posterior (A-P) limb patterning involves a common set of cell types and tissues, producing distinct skeletal morphologies that are not based in cell fate changes per se. Understanding how Shh specifies limb skeletal pattern is both central to the problem of structural morphogenesis and relevant to regenerative medicine. Shh is secreted by posterior limb bud mesoderm cells defined functionally as the "zone of polarizing activity" (ZPA) and regulates the specification of distinct A-P digit types (d2-d5)[12], excepting digit 1, which forms in the absence of Shh[11]. Patterning is coupled with growth and, during its 2-day limb bud expression (Figure 1a), Shh regulates both digit types and numbers and is functionally highly conserved across tetrapod vertebrates[1].

Yet, despite intense investigation for over two decades, the mechanism by which Shh patterns digits remains controversial. Very disparate models have been proposed in different species that otherwise share similar gene regulatory networks governing limb development[1-4,6,7]. Morphogen-based models of Shh function derive from chick studies showing that changes in concentration or exposure duration can alter both the number and the types of digits specified, with the most posterior identities requiring the highest concentrations or longest exposure[2,3,5,6]. Lineage tracing of ZPA-descendant cells in both chick and mouse revealed that digits 4 and 5 (d4,d5) arise from limb cells that previously expressed Shh[4,13], leading to the proposal that temporal integration of short-range Shh, rather than long-range graded signaling, specifies different digit types. More anterior cells become displaced away from the ZPA during A-P expansion, while Shh-expressing digit progenitors (d4,d5) remain, receiving the longest exposure[4]. A variant of this temporal-expansion model proposed that Shh patterning and proliferation roles are integrated and digit progenitors become "promoted" successively to more posterior identities by continued Shh exposure during expansion[6]. However, genetic lineage tracing of Shh response indicates that Shh-expressing ZPA cells become refractory to Shh over time[10], seemingly at odds with temporal integration and promotion models. We previously interrogated the temporal requirements for Shh function in mouse limb using a conditional *Shh*-mutant[7] and found *Shh* was required over a limited (~8h) interval to specify normal digits;

subsequent *Shh* removal resulted in progressive digit loss that reflected the normal temporal order in which they arise, rather than their A-P position. We proposed a biphasic model in which Shh is required only briefly, perhaps as a spatial morphogen, for patterning (early phase), but over an extended time period to promote survival and expansion of digit progenitors (late phase).

Results:

A transient Shh pulse restores normal limb development with enforced cell survival.

To test the biphasic model critically, we used a genetic strategy to uncouple the Shh requirement in digit patterning from growth, by enforcing cell survival to substitute for Shh late-phase function, and assessed digit formation. The pro-apoptotic *Bax*/*Bak* genes[14] were deleted in *Shh* conditional mutant limb buds exposed to only a transient early Shh pulse (using $Shh^{C/C}$;Hoxb6CreER allele hereafter referred to as *Shh*-CKO, and $Bax^{C/C}$;$Bak^{-/-}$ alleles referred to as *Bax*-CKO; see extended data Table 1 for complete list of all crosses and genotypes used). Tamoxifen injection time to delete *Shh* was optimized (to E9.5+3hrs, Figure 1) so that *Shh*-CKO retaining one wild-type *Bax* allele (cell survival not restored) invariably displayed a *Shh* germ-line null ($Shh^{-/-}$) skeletal phenotype (28/28). This tamoxifen treatment (E9.5+3h, Figure 1b, extended data Figure 1a) precedes the normal *Shh* expression onset by about 8 hours; Shh activity in tamoxifen-treated embryos was reported by measuring direct Shh target RNAs (*Gli1*, *Ptch1*)[8,9,15] at 2-hour (~one somite) intervals post-tamoxifen (Figure 1b, extended data Figure 1a). A transient 2-3 hour Shh activity window was detected in approximately half of the *Shh*-CKO embryos (7/15 *Ptch1*, 4/10 *Gli1*, Figure 1b, extended data figure 1a); no activity was detected in the other half.

Notably, limb bud cell survival was completely restored in 100% (11/11) of *Bax*-CKO embryos (extended data Figure 1b), but the *Bax*-CKO alone had no phenotypic effect on limb skeletal patterning ($Shh^{+/C}$;*Bax*-CKO, Figure 1c). In *Shh*-CKO;*Bax*-CKO embryos, blocking cell death rescued formation of from 3 to 5 digits with normal morphology in about half the embryos (18/31), while the remaining 50% retained the $Shh^{-/-}$ null mutant limb phenotype (Figure 1c), correlating well with the fraction of embryos that displayed transient, early Shh activity (Figure 1b, extended data Figure 1a, Table 1). Half of the embryos lack any transient Shh expression and

are expected to generate a Shh null skeletal phenotype, as observed (13/31). In *Shh*-CKO;*Bax*-CKO embryos with rescued limbs (18/31), normal long bone morphology (tibia/fibula; zeugopod) was also restored (see also Figure 2c), and normal A-P polarity was clearly evident in both the long bones and digits, including distinctive d1 and d5 identities. In contrast, all (100%) of sibling *Shh*-CKO embryos retaining one functional *Bax* allele (*Shh*-CKO;$Bax^{+/C}$) had a *Shh* null limb phenotype with a single dysmorphic digit and malformed zeugopod (28/28, Figure 1c).

These data indicate that a transient early Shh pulse (~2-3h) suffices to specify digit progenitors, but not to maintain progenitor cell survival. We next asked if a short Shh pulse is even necessary to specify digit progenitors if cell survival is enforced, using crosses with a non-conditional *Shh* null mutant completely devoid of any Shh activity ($Shh^{-/-}$;*Bax*-CKO; Figure 1c). Cell death was completely blocked (9/9, extended data Figure 1b), but enforced cell survival failed to rescue any digit or normal long bone formation in $Shh^{-/-}$;*Bax*-CKO limbs (0/18, Figure 1c, extended data Table 1), even using non-conditional *Bax/Bak* mutant alleles ($Shh^{-/-}$;$Bax^{-/-}$;$Bak^{-/-}$) to ensure complete *Bax/Bak* inactivation in $Shh^{-/-}$ (0/6 skeletal rescue; extended data Table 1). These results indicate that an early, transient Shh pulse is both necessary and sufficient to specify normal digit and long bone formation. After this transient pulse, sustained Shh activity can be substituted by *Bax/Bak* removal, implying that later stage Shh acts mainly to support cell survival and limb bud expansion.

Rescue of Shh loss by enforced cell survival is not due to Hh pathway re-activation.

Biochemical and functional analyses of *Shh*-CKO;*Bax*-CKO embryos established that the observed rescue of normal limb development was not due to Shh pathway re-activation. First, assay of direct Shh target *Ptch1* (0/7, 0/9) and *Gli1* (0/7) RNAs at early and late patterning stages failed to detect any Hh ligand or pathway recovery in *Shh*-CKO;*Bax*-CKO embryos (Figure 2a, extended data Figure 2). Shh prevents processing of Gli2/Gli3 nuclear effectors from full-length activators (Gli2FL/Gli3FL; GliA) to truncated repressors (Gli2R/Gli3R) of Shh targets[16-18]. Release from Gli3 repression plays the main role in most Shh limb target regulation[8,9,19]. Consequently, key limb target activation may occur ligand-independently without reporter activation via Gli3R removal or functional antagonism[20,21]. *Hand2*, which induces ZPA/Shh by antagonizing Gli3[22], is directly repressed by Gli3R[15] and remained absent from rescued *Shh*-CKO;*Bax*-CKO early (10/10) and later

(10/11) stage limb buds (Figure 2a).

Gli3R activity can also be modulated at the protein level, by altered processing or degradation[16,18]. Although *Bax/Bak* removal in wildtype limb buds has no impact on skeletal patterning, pro-survival Bcl2 family members sequester SuFu, a negative Hh pathway modulator, away from its Gli-processing activity[23]. *Bax/Bak* removal could elevate the free Bcl2 pool to generate a Gli3R deficit, rescuing *Shh* mutant limbs. We examined Gli3 protein levels in early individual limb buds (E10.75, Figure 2b). Gli3FL/Gli3R ratios in *Shh*-CKO;*Bax*-CKO were unchanged from *Shh*$^{-/-}$;*Bax*-CKO limb buds, and both were equally reduced compared to Shh-expressing controls (Figure 2b), indicating that rescue was not secondary to reduced Gli3R protein levels.

To assess if the "effective" repressor activity of Gli3R protein might be altered in rescued limb buds without quantitative changes[20,21], we compared the effect of *Bax/Bak* removal with genetic *Gli3* dosage reduction in both *Shh*-CKO and *Shh*$^{-/-}$ limbs. Complete *Gli3* loss alone rescues limb development in *Shh*$^{-/-}$ embryos[8,9], albeit with synpolydactyly. However, reduced *Gli3* dosage (*Shh*$^{-/-}$;*Gli3*$^{+/-}$) has a modest phenotypic effect (Figure 2c). In the *Shh*$^{-/-}$ with loss of one *Gli3* allele, zeugopod morphology was improved and several small digit rudiments formed (*Gli3*+/-, 8/8); in contrast, no change in the *Shh*$^{-/-}$ phenotype was observed when only *Bax/Bak* was removed (*Bax*-CKO, 0/18, compare Figures 2c and 1c). Furthermore, removing *Bax/Bak* in the *Shh*$^{-/-}$;*Gli3*$^{+/-}$ limb did not improve limb skeletal phenotype beyond the effect of *Gli3* dosage reduction alone (Figure 2c, 10/10), suggesting that *Bax/Bak* removal did not impact “effective” Gli3R levels significantly. Whereas *Bax/Bak* removal had little effect but *Gli3* dosage had a profound effect on the *Shh*$^{-/-}$, the reverse holds for the *Shh*-CKO (see arrows, Figure 2c). The *Shh*-CKO;*Gli3*$^{+/-}$ was phenotypically identical to the *Shh*$^{-/-}$;*Gli3*$^{+/-}$ (12/12; Figure 2c). In contrast, in *Shh*-CKO;*Bax*-CKO limbs both zeugopod and between 3-5 digits with normal morphologies and clear A-P polarity were restored (18/31; Figures 1c, 2c). Together, these results argue strongly against altered Gli3R function per se as a mechanistic basis for rescue of normally polarized limb development in the early *Shh*-CKO by enforced cell survival.

Expression of outgrowth and patterning regulators is sustained in early Shh-CKO with enforced cell survival.

To understand how digit patterning is restored by transient Shh exposure, we examined expression of major downstream targets that regulate limb bud outgrowth (AER/Fgf signaling[24,25]) and digit patterning (5'*Hox* genes[26-29]). Unlike *Hand2* and direct GliA targets (*Ptch1*, *Gli1*), their expression is maintained in a subset of *Shh*-CKO;*Bax*-CKO embryos, roughly correlating with observed 50% frequencies of detectable transient Shh activity early, and skeletal rescue at late stages (Figures 1,2, extended data Figures 1,2). In the remainder, expression profiles in *Shh*-CKO;*Bax*-CKO resembled that of *Shh*$^{-/-}$;*Bax*-CKO (Figure 2, extended data Figure 2).

In the null *Shh*$^{-/-}$, hindlimb *Fgf8* expression declines after E10.5[11], related to loss of the direct Shh target *Grem1*, which plays a key role in AER/Fgf8 maintenance[25]. *Shh*$^{-/-}$;*Bax*-CKO limb buds likewise lacked early and late *Grem1* expression (absent in 5/5 and 4/4, Figure 2a) and by E11.5 had clearly reduced *Fgf8* expression (3/3, extended data Figure 2). In contrast, a subset of *Shh*-CKO;*Bax*-CKO embryos retained early and late *Grem1* expression (4/10 and 3/7, Figure 2a), and maintained *Fgf8* late (3/7, extended data Figure 2). The Fgf8-regulated target, *Cyp26b1*, required for retinoic acid clearance to enable distal limb bud progression[30], was also maintained in *Shh*-CKO;*Bax*-CKO (4/6) but declined in *Shh*$^{-/-}$;*Bax*-CKO by E11.5 (3/3, extended data Figure 2). *Jag1*, a direct target that marks Shh-dependent early mesenchymal limb progenitors[31,32], failed to be expressed in *Shh*$^{-/-}$;*Bax*-CKO (4/4), but expression was maintained in a subset of *Shh*-CKO;*Bax*-CKO limb buds both early and late (2/6 and 2/5, extended data Figure 2).

Several 5'*Hox* genes regulate patterning downstream of Shh[26,28]. *Hoxd13* and *Hoxa13*, critical for digit specification[27,29], are both expressed only at late stages and at low levels in *Shh*$^{-/-}$;*Bax*-CKO (3/3, 4/4) compared to controls (Figure 2a, extended data Figure 2). Low level distal *Hoxa13* expression was already detected early in a fraction of *Shh*-CKO,*Bax*-CKO hindlimb buds (6/10), and became robust at later stages (5/8, Figure 2a). *Hoxd13* expression was absent early, but was clearly detected at the onset of the distal footplate 5'*Hoxd* expansion phase[33] (4/7, E11.5, Figure 2a), well prior to the late digit condensation stage expression at E12.5 that resumes in both the *Shh*$^{-/-}$ null[11] and *Shh*$^{-/-}$;*Bax*-CKO (extended data Figure 2). *Hox11* paralogs play a key role in

zeugopod patterning and growth[34], which is also highly perturbed in the *Shh*$^{-/-}$ but restored in *Shh*-CKO;*Bax*-CKO hindlimbs (tibia/fibula, Figure 1c). While early *Hoxd11* expression in *Shh*$^{-/-}$;*Bax*-CKO (2/2) was similar to controls the second phase distal expansion was undetectable (2/2). In contrast, *Hoxd11* was maintained at control levels both early and late in a subset of *Shh*-CKO;*Bax*-CKO limb buds (5/5, 2/7, extended data Figure 2). Shh inhibition in short term mouse limb bud cultures suggested that some Shh targets are maintained if Shh activity is curtailed, as we showed here (eg. *Grem1*, *Jag1*), but others, particularly 5'*Hoxd* genes, require sustained Shh activity for their continued expression[19,32]. Yet we found that second phase distal 5'*Hoxd* expansion was preserved in about half of *Shh*-CKO;*Bax*-CKO embryos, correlating well with the fraction displaying early transient Shh activity and late skeletal rescue. Normal development does not progress in short-term limb bud cultures, precluding analysis of the 5'*Hoxd* second phase following early Shh removal. 5'*Hoxd* genes act mainly during this distal expansion phase to determine digit identity by regulating late stage interdigit signaling centers[35], so the sustained late phase 5'*Hoxd* activation likely suffices for morphogenesis of normal distinct digit types in *Shh*-CKO;*Bax*-CKO embryos.

These results indicate that expression of targets important for both limb bud outgrowth and patterning are sustained by a transient pulse of Shh with enforced cell survival, providing a basis for the phenotypic rescue of limb development, but do not address the issue of how transient Shh activity leads to stable, A-P-graded target expression in the limb.

Rescued digits in the early Shh-CKO arise from cells that have not responded directly to Shh.

The short 2-3h pulse of Shh activity required for normal limb development if cell survival is enforced is not readily explained by temporal signal integration models. However, this short time window could still be compatible with transient activity of a spatially graded morphogen. Transient, pre-steady state morphogen effects, operating at onset of a signaling gradient, have been proposed and experimentally validated for Hh signaling in the *drosophila* wing disc [36]. To determine if Shh signals as a long-range morphogen during this early time window, we compared the lineage of Shh-producing/ZPA and Shh-responding cells present at early stages immediately after *Shh* expression onset during normal development.

We performed lineage tracing using crosses that include both *Shh*$^{CreER/+}$ and *Gli1*$^{CreER/+}$ knock-in alleles to genetically mark cells (RosaLacZ reporter activation; Fig 3a) that had either produced or responded to Shh signal, respectively[4,10]. Sibling embryos that expressed a single CreER allele were analyzed from the same litter, to ensure Shh production-response comparisons at identical embryonic ages and tamoxifen exposure times. A single tamoxifen dose was given at closely spaced early times spanning *Shh* expression onset (Figure 3b); limb buds were collected at E12.5-13.5, after digit rays formed and descendant cell contributions to different digit condensations (*LacZ*+) could be easily scored (Figure 3a).

Surprisingly tamoxifen-induced Cre activation revealed that, at early times (when a transient Shh pulse with enforced cell survival restores normal limb development), Shh only acts very short-range. For tamoxifen treatment prior to E10.25, Shh response (Gli1CreER activity) was confined to cells that later give rise to digits 4 and 5 (Figure 3a). Longer-range signaling was not detected until later tamoxifen-induction times, initially extending toward digit 3 (E10.25) and later also including digit 2 (E10.5) territories (Figure 3a). However, tamoxifen treatment at a much earlier stage, E9.5+3h (Fig 1b), provides a transient Shh pulse that is both necessary and sufficient to specify formation of all 5 digits if cell survival is enforced. During this time interval, the lineage tracing results demonstrate that Shh activity acts only short-range; Shh response is limited to the Shh-producing ZPA, and can only directly impact progenitors giving rise to digits 4-5. Consequently, other "Shh-dependent" digit progenitors must respond indirectly to downstream Shh targets that act non-autonomously, implying an indirect relay mechanism (Figure 3b-blue). Notably however, at later stages Shh does act as a long-range signal (E10.5, Figure 3a,b-green-hatched), apparently in its role supporting cell survival.

Shh is required indirectly to specify digit 1 (thumb).

To test if Shh acts via a relay to specify non-ZPA digits, we used a genetic strategy (diagrammed in Figure 4a) to activate Shh targets autonomously only in the ZPA and ask if any non-ZPA-derived digits are rescued in the complete absence of Shh ligand (*Shh* null). Cell-autonomous pathway activation was achieved using a constitutively-active form of Smoothened (SmoM2), a membrane

GPCR essential for Shh pathway transduction[37]. The *Shh*^{Cre} knock-in allele[4] was used to activate expression of a conditional SmoM2 transgene (*Rosa*^{SmoM2})[38], restricting SmoM2 and Shh target activation to the ZPA (*Shh*^{cre};*Rosa*$^{SmoM2/+}$; referred to as Shh-SmoM2+), and evaluated in the *Shh* null background (*Shh*$^{cre/-}$).

Enforced Shh-response by SmoM2 in the ZPA affects Ihh-regulated targets and cartilage differentiation[39], precluding morphologic evaluation of posterior, ZPA-descendant (d4,d5) digits. However, in otherwise "wildtype" embryos, Shh-SmoM2+ (*Shh*$^{cre/+}$;*Rosa*$^{SmoM2/LacZ}$) did not alter normal morphology/identity of non-ZPA digits (d1-d3) in most embryos (60/64). In a small percentage (~5%; 4/64), anterior digit duplications occurred, associated with induction of an ectopic, anterior Shh/ZPA focus (detected by *Rosa*^{LacZ} reporter; extended data Figure 3a). Unexpectedly, enforced cell-autonomous pathway activation in the ZPA of *Shh*$^{cre/-}$;Shh-SmoM2 rescued formation of a morphologically normal digit 1 at high frequency (60-70%; 21/32 limbs) in both *Shh*$^{cre/-}$ fore- and hindlimbs (Figure 4b). This rescued "digit 1" was not ZPA-derived (LacZ reporter-negative), but arose from anterior limb bud progenitors (5/5; Figure 4c), and was unrelated to cryptic Ihh or Dhh ligand or downstream pathway activation (Gli1 - 0/8; Ptch1 - 0/10; extended data Figure 3c).

Digit 1 specification is thought to be Hh-independent, based on a persistent digit 1-like structure in *Shh* null hindlimbs[11] and the normal lack of direct Shh-response in the digit 1 progenitor territory[10] (see also Figure 3). However, whereas our lineage analysis clearly demonstrates that the morphological digit 1 rescued in the *Shh*$^{cre/-}$;Shh-SmoM2 arises from anterior non-ZPA limb cells, we found that the single dysmorphic digit present in the *Shh* null mutant (*Shh*$^{cre/-}$) is actually descended from posterior ZPA (LacZ+) d4/d5 progenitor cells (Figure 4c, extended data Figure 3a). Consistent with digit 1 identity, *Hoxa13*, which is critical for digit 1 specification[27,29,40], and is absent or greatly reduced in *Shh*$^{Cre/-}$ (0/4, Figure 4d, forelimb shown), was restored across the distal limb bud in the *Shh*$^{cre/-}$;Shh-SmoM2+ (6/6; Figure 4d). A late digit 1-specific marker (*Uncx4.1*) was also expressed in the rescued digit domain of *Shh*$^{cre/-}$;Shh-SmoM2 (6/8), but not in *Shh*$^{Cre/-}$ (0/4; extended data Figure 3b). Together, these results strongly argue that a bona fide digit 1 is restored in the *Shh*$^{cre/-}$;Shh-SmoM2, and indicate that digit 1 specification is actually Shh-

dependent, requiring an indirect signal activated downstream of Shh-response in the ZPA.

Several factors may explain why digit 1, but not other non-ZPA digits (digit 2,3) were restored by Shh-SmoM2. Shh function in cell survival is still absent, and considerable apoptosis still present in the *Shh*$^{cre/-}$;Shh-SmoM2+ limb buds (extended data Figure 3d), but enforcing cell survival (*Shh*$^{Cre/-}$;*Bax*$^{-/-}$;*Bak*$^{-/-}$;Shh-SmoM2+; extended data Table 1) did not rescue any further digit formation besides digit 1 (8/8). Failure to rescue digits 2-3 may reflect a requirement for an early proliferative signal that is not restored, and/or a problem inherent in the timing of enforced Shh-response in ZPA cells (induced by *Shh*^{Cre} only after normal *Shh* expression onset). Additionally, activation is restricted to Shh-producing cells, which are mosaic in the early ZPA (Figure 3a); complete relay signaling may require target activation in adjacent non-Shh producing cells within the ZPA region. The *SmoM2* allele also results in uniform, non-physiologic levels of autonomous pathway activation that might interfere with some normal target gene expression requiring different Shh activity levels.

DISCUSSION:

Our genetic rescue reveals two distinct roles for Shh in the limb: a transient (2-3hr), early requirement that is critical to specify all digits, and a sustained requirement to promote cell survival. This transient Shh pulse is both necessary and sufficient for normal limb morphogenesis, if the role of Shh in maintaining cell survival is substituted (*Bax/Bak* removal). Yet genetic lineage tracing shows that Shh acts only short-range and Shh-response is restricted to ZPA-derived digit progenitors (d4-d5) during the same time interval that suffices to specify all digits, indicating that Shh does not act as a limb morphogen and that non-ZPA digits (d1-3) are specified indirectly by a Shh-induced signal relay (Figure 4e). Furthermore, although the digit 4/5 territory (ZPA) responds directly to Shh signaling early, digit 4/5 specification likewise requires only transient Shh exposure. Unexpectedly, long-range Shh signaling occurs only at later limb bud stages and acts to sustain cell survival across the digit 2-5 territories. This late stage signaling over extended distances may be facilitated by filopodia capable of transporting Shh ligand long-range in limb bud[41].

Uncovering the mechanisms that sustain gene activation after transient Shh exposure will be an

important future focus to illuminate how Shh patterns the developing limb. Stable alterations in target gene expression following transient Shh exposure could involve several, non-mutually exclusive mechanisms including chromatin and/or DNA modifications and relay mechanisms incorporating lock-on circuitry[42]. Target de-repression plays a major role in the limb, and recent work suggests that Shh targets are poised for expression as soon as Gli3-mediated repression is alleviated[43]. A transient burst of Shh activity could trigger a self-reinforcing bi-stable switch[42] if activating factors that reinforce target expression also block re-introduction of repressive marks by Gli3R. Furthermore, our results clearly implicate non-cell autonomous relay signals that act downstream of transient Shh activity to specify non-ZPA derived digits. Relay signals can become self-sustaining through either double-positive or double-negative feedback loops. For example, Tbx5 is required only transiently in the limb to initiate a self-sustaining Fgf10-Fgf8 positive feedback loop[44,45].

Digit identity is morphologic in nature, arising in distinct organization of the same tissues and not based in cell fate differences, features suggesting progressive specification. Indeed, work in both chick and mouse models indicates that late interdigit signaling centers[35,46-48] impinge on digit tip progenitors to regulate phalanx formation and determine final digit identities. Shh may regulate digits specified at particular A-P limb positions through relay signals that establish late signaling centers (Figure 4e). Yet, a relay mechanism is incompatible with Shh acting either as a traditional morphogen or by temporal integration, as supported by gain-of-function chick studies showing graded effects[1-3]. Loss-of-function chick studies entail cyclopamine[5,6,49], which blocks all Hedgehog ligands, and whose effects in ovo extend from early Shh into phalanx-forming stages (see Figure 3 in ref.[49]), also affecting digit tip Ihh expression. Reduced *Ihh* causes phalangeal loss phenotypes[48,50] that can score as digit identity changes attributed to Shh loss. Reduced cell survival due to Shh inhibition in these experiments may also impact late-stage digit morphogenesis (phalanx formation). Notably, some chick studies have also suggested a role for relay mechanisms in Shh signaling; in particular, a membrane-tethered Shh ligand could still induce posterior digit formation at a distance[3], and several papers have implicated Bmps as secondary signals modulating digit identity downstream of Shh[2,47,51]. The discrepancy between mouse and chick remains to be explored.

Our genetic assay for relay signals revealed that digit 1 (d1), like other anterior digits (d2,d3), is actually Shh-dependent. But previous work clearly demonstrated that direct Shh signaling selectively prevents formation of d1 territory, and that a complex regulatory circuit repressing *Shh* expression-response in the anterior limb bud is essential for d1 specification[1,52,53]. In contrast to other digits specified by Shh-induced relay signals, the digit 1 territory remains outside the range of Shh signaling response during the entire expansion phase when Shh maintains cell survival, which must be sustained differently. Why impose such a complex regulatory hierarchy for d1 specification (Figure 4e), involving repression by direct Shh signaling, but requiring an indirect Shh-dependent relay signal? We propose that the unique control and consequent delay in d1 specification enabled its independent evolution by uncoupling its regulation and morphogenesis from that governing other digits. Such regulatory uncoupling would facilitate the evolution of an opposable thumb, as well as related grasping/clutching adaptations important for arboreal tetrapods, including birds and mammals.

Methods

Mouse lines and tamoxifen injection:

All animal studies were carried out according to the ethical guidelines of the Institutional Animal Care and Use Committee (IACUC) at NCI-Frederick under protocol #ASP-17-405. The *Shh*-floxed[54], *Shh* null[55], *Bax*-flox;*Bak*$^{-/-}$[14], and *Gli3* (*Xt-J*)[56] mutant lines, and the *Hoxb6*CreER[57], *Shh*Cre, *Shh*CreER[4], *Gli1*CreER[10], *Rosa*SmoM2[38], *Rosa*LacZ[58], and *Rosa*EYFP[59] mouse lines were all described previously. *Bax*-deleted (*Bax*$^{+/-}$) mice were generated by crossing *Bax*-flox males with *Prrx1*Cre[60] females to produce germ-line recombination. A detailed summary of the crosses used to generate embryos for different experiments and outcomes is provided in extended data Table 1. For timed matings, noon on the date of the vaginal plug was defined as E0.5. For phenotypic rescue with *Hoxb6*CreER, pregnant mice were injected intraperitoneally with a single dose of 3mg tamoxifen (Sigma, T-5648) and 1mg progesterone[61] (Watson, NDC 0591-3128-79) at E9.5+3hrs and embryos were collected at times indicated. For lineage tracing with *Shh*CreER and *Gli1*CreER, a single dose of 0.5mg tamoxifen was injected at the times indicated.

Whole mount in situ hybridization:

Hybridizations were carried out following a previously described detailed protocol[62]. Embryos were fixed in 4% paraformaldehyde overnight, washed in PBS, gradually changed to absolute methanol and bleached with 5% H_2O_2. Embryos with different genotypes were treated together, in one tube, with 20ug/ml proteinase K for 8-16 mins based on the embryo age (this step was omitted for *Fgf8* probe). Gene-specific, digoxigenin-UTP labeled probes were synthesized from cDNA templates, and incubated with embryos in hybridization buffer with 50% formamide overnight at 70^{o}C. The embryos were then washed with a series of buffers and incubated in alkaline-phosphatase-conjugated anti-digoxigenin antibody overnight at 4^{o}C. After washing with 0.1% Tween in Tris buffered saline, embryos were incubated in BM purple (Sigma, 11442074001) to detect hybridized RNA.

Skeletal staining:

For skeletal staining[63], embryos were collected at E15.5-E18.5 and fixed in absolute ethanol

overnight, followed by acetone overnight, and by staining in alcian blue/alizarin red in 95% ethanol overnight. After clearing in 1% KOH in H_2O for several hours followed by 1% KOH in 20% glycerol, embryos were stored and imaged in 50% glycerol.

Lysotracker staining:

Embryos were collected in PBS and immediately incubated in lysotracker red (Sigma) in PBS with calcium and magnesium for 30 mins at 37°C. Embryos were then washed in PBS and fixed in 4% paraformaldehyde overnight at 4°C. Embryos were washed in PBS, transferred to absolute methanol in graded steps and cleared in benzyl alcohol/benzyl benzoate (BABB) solution to visualize staining.

Western blot and quantification analysis:

For western blot analysis, hindlimb buds from individual E10.75 embryos were dissected and lysed in 1x NuPAGE LDS sample buffer with 2% SDS and proteinase inhibitors. Reducing agent was added and samples were heated to 95 °C for 10 mins before loading. Two hindlimb buds (from 1 embryo) were loaded per lane, and electrophoresed in NuPAGE 3-8% Tris-Acetate protein gels. Proteins transferred to nitrocellulose membranes were probed with either affinity-purified polyclonal rabbit anti-Gli3[20] or goat polyclonal anti-Gli3 (R&D, AF3690) and mouse anti-vinculin (Sigma, V9264) and visualized with fluorescent secondary antibodies (LI-COR IRDye 800CW, 926-32211, anti-rabbit green; 926-32214, anti-goat green; and with #680RD, #926-68072, anti-mouse red) using LI-COR Odyssey CLx. Bands were quantified with Image Studio software.

Beta-galactosidase (LacZ) staining:

Embryos were fixed in 2% paraformaldehyde with 0.2% glutaraldehyde for 1h, washed in PBS with 0.1% Tween and stained with XGal (1mg/ml) in PBT and 2mM $MgCl_2$, 5mM Ferro-CN, 5mM Ferri-CN, at 37 °C for several hours.

Acknowledgements:

We thank Cliff Tabin for stimulating discussions; Heinz Arnheiter, Denis Duboule, Bernhard Herrmann, Alex Joyner, Marie Kmita, Peter Koopman, Gail Martin, Marian Ros, Scott Stadler and Yingzi Yang for providing probes; and Sohyun Ahn, Chin Chiang, Alex Joyner, Andy McMahon, Cliff Tabin, Heiner Westphal and Yingzi Yang for providing mouse lines. This research was supported by the Center for Cancer Research (SM, intramural Research Program), National Cancer Institute, NIH.

Author Contributions SM and JZ designed the project and wrote the paper, and JZ, AT, and BDH performed the experiments.

Author information Correspondence and requests for material should be addressed to SM (mackems@mail.nih.gov). The authors declare no competing financial interests.

REFERENCES:

1 Zhu, J. & Mackem, S. John Saunders' ZPA, Sonic hedgehog and digit identity - How does it really all work? *Dev Biol* **429**, 391-400, doi:10.1016/j.ydbio.2017.02.001 (2017).

2 Drossopoulou, G. *et al.* A model for anteroposterior patterning of the vertebrate limb based on sequential long- and short-range Shh signalling and Bmp signalling. *Development* **127**, 1337-1348 (2000).

3 Yang, Y. *et al.* Relationship between dose, distance and time in Sonic Hedgehog-mediated regulation of anteroposterior polarity in the chick limb. *Development* **124**, 4393-4404 (1997).

4 Harfe, B. D. *et al.* Evidence for an expansion-based temporal Shh gradient in specifying vertebrate digit identities. *Cell* **118**, 517-528, doi:Doi 10.1016/J.Cell.2004.07.024 (2004).

5 Scherz, P. J., McGlinn, E., Nissim, S. & Tabin, C. J. Extended exposure to Sonic hedgehog is required for patterning the posterior digits of the vertebrate limb. *Dev Biol* **308**, 343-354, doi:10.1016/j.ydbio.2007.05.030 (2007).

6 Towers, M., Mahood, R., Yin, Y. & Tickle, C. Integration of growth and specification in chick wing digit-patterning. *Nature* **452**, 882-886, doi:10.1038/nature06718 (2008).

7 Zhu, J. *et al.* Uncoupling Sonic hedgehog control of pattern and expansion of the developing limb bud. *Dev Cell* **14**, 624-632, doi:10.1016/j.devcel.2008.01.008 (2008).

8 Litingtung, Y., Dahn, R. D., Li, Y., Fallon, J. F. & Chiang, C. Shh and Gli3 are dispensable for limb skeleton formation but regulate digit number and identity. *Nature* **418**, 979-983, doi:10.1038/nature01033 (2002).

9 te Welscher, P. *et al.* Progression of vertebrate limb development through SHH-mediated counteraction of GLI3. *Science* **298**, 827-830, doi:10.1126/science.1075620 (2002).

10 Ahn, S. & Joyner, A. L. Dynamic changes in the response of cells to positive hedgehog signaling during mouse limb patterning. *Cell* **118**, 505-516, doi:10.1016/j.cell.2004.07.023 (2004).

11 Chiang, C. *et al.* Manifestation of the limb prepattern: limb development in the absence of sonic hedgehog function. *Dev Biol* **236**, 421-435, doi:10.1006/dbio.2001.0346 (2001).

12 Riddle, R. D., Johnson, R. L., Laufer, E. & Tabin, C. Sonic hedgehog mediates the polarizing activity of the ZPA. *Cell* **75**, 1401-1416, doi:10.1016/0092-8674(93)90626-2 (1993).

13 Towers, M., Signolet, J., Sherman, A., Sang, H. & Tickle, C. Insights into bird wing evolution and digit specification from polarizing region fate maps. *Nat Commun* **2**, 426, doi:10.1038/ncomms1437 (2011).

14 Takeuchi, O. *et al.* Essential role of BAX,BAK in B cell homeostasis and prevention of autoimmune disease. *Proc Natl Acad Sci U S A* **102**, 11272-11277, doi:10.1073/pnas.0504783102 (2005).

15 Vokes, S. A., Ji, H., Wong, W. H. & McMahon, A. P. A genome-scale analysis of the cis-regulatory circuitry underlying sonic hedgehog-mediated patterning of the mammalian limb. *Genes Dev* **22**, 2651-2663, doi:10.1101/gad.1693008 (2008).

16 Pan, Y., Bai, C. B., Joyner, A. L. & Wang, B. Sonic hedgehog signaling regulates Gli2 transcriptional activity by suppressing its processing and degradation. *Mol Cell Biol* **26**, 3365-3377, doi:10.1128/MCB.26.9.3365-3377.2006 (2006).

17 Wang, B., Fallon, J. F. & Beachy, P. A. Hedgehog-regulated processing of Gli3 produces an anterior/posterior repressor gradient in the developing vertebrate limb. *Cell* **100**, 423-434, doi:10.1016/s0092-8674(00)80678-9 (2000).

18 Wang, C., Pan, Y. & Wang, B. Suppressor of fused and Spop regulate the stability, processing and function of Gli2 and Gli3 full-length activators but not their repressors. *Development* **137**, 2001-2009, doi:10.1242/dev.052126 (2010).

19 Lewandowski, J. P. *et al.* Spatiotemporal regulation of GLI target genes in the mammalian limb bud. *Dev Biol* **406**, 92-103, doi:10.1016/j.ydbio.2015.07.022 (2015).

20 Chen, Y. *et al.* Direct interaction with Hoxd proteins reverses Gli3-repressor function to promote digit formation downstream of Shh. *Development* **131**, 2339-2347, doi:10.1242/dev.01115 (2004).

21 Galli, A. *et al.* Distinct roles of Hand2 in initiating polarity and posterior Shh expression during the onset of mouse limb bud development. *PLoS Genet* **6**, e1000901, doi:10.1371/journal.pgen.1000901 (2010).

22 te Welscher, P., Fernandez-Teran, M., Ros, M. A. & Zeller, R. Mutual genetic antagonism involving GLI3 and dHAND prepatterns the vertebrate limb bud mesenchyme prior to SHH signaling. *Genes Dev* **16**, 421-426, doi:10.1101/gad.219202 (2002).

23 Wu, X. *et al.* Extra-mitochondrial prosurvival BCL-2 proteins regulate gene transcription by inhibiting the SUFU tumour suppressor. *Nat Cell Biol* **19**, 1226-1236, doi:10.1038/ncb3616 (2017).

24 Mariani, F. V., Ahn, C. P. & Martin, G. R. Genetic evidence that FGFs have an instructive role in limb proximal-distal patterning. *Nature* **453**, 401-405, doi:10.1038/nature06876 (2008).

25 Zuniga, A., Haramis, A. P., McMahon, A. P. & Zeller, R. Signal relay by BMP antagonism controls the SHH/FGF4 feedback loop in vertebrate limb buds. *Nature* **401**, 598-602, doi:10.1038/44157 (1999).

26 Davis, A. P. & Capecchi, M. R. A mutational analysis of the 5' HoxD genes: Dissection of genetic interactions during limb development in the mouse. *Development* **122**, 1175-1185 (1996).

27 Fromental-Ramain, C. *et al.* Hoxa-13 and Hoxd-13 play a crucial role in the patterning of the limb autopod. *Development* **122**, 2997-3011 (1996).

28 Zakany, J. & Duboule, D. Synpolydactyly in mice with a targeted deficiency in the HoxD complex. *Nature* **384**, 69-71 (1996).

29 Stadler, H. S., Higgins, K. M. & Capecchi, M. R. Loss of Eph-receptor expression correlates with loss of cell adhesion and chondrogenic capacity in Hoxa13 mutant limbs. *Development* **128**, 4177-4188 (2001).

30 Probst, S. *et al.* SHH propagates distal limb bud development by enhancing CYP26B1-mediated retinoic acid clearance via AER-FGF signalling. *Development* **138**, 1913-1923, doi:10.1242/dev.063966 (2011).

31 Reinhardt, R. *et al.* Molecular signatures identify immature mesenchymal progenitors in early mouse limb buds that respond differentially to morphogen signaling. *Development* **146**, dev173328, doi:10.1242/dev.173328 (2019).

32 Panman, L. *et al.* Differential regulation of gene expression in the digit forming area of the mouse limb bud by SHH and gremlin 1/FGF-mediated epithelial-mesenchymal signalling. *Development* **133**, 3419-3428, doi:10.1242/dev.02529 (2006).

33 Tarchini, B. & Duboule, D. Control of Hoxd genes' collinearity during early limb development. *Dev Cell* **10**, 93-103, doi:10.1016/j.devcel.2005.11.014 (2006).

34 Davis, A. P., Witte, D. P., Hsieh-Li, H. M., Potter, S. S. & Capecchi, M. R. Absence of radius and ulna in mice lacking hoxa-11 and hoxd-11. *Nature* **375**, 791-795, doi:10.1038/375791a0 (1995).

35 Huang, B. L. *et al.* An interdigit signalling centre instructs coordinate phalanx-joint formation governed by 5'Hoxd-Gli3 antagonism. *Nat Commun* **7**, 12903, doi:10.1038/ncomms12903 (2016).

36 Nahmad, M. & Stathopoulos, A. Dynamic interpretation of hedgehog signaling in the Drosophila wing disc. *PLoS Biol* **7**, e1000202, doi:10.1371/journal.pbio.1000202 (2009).

37 Kong, J. H., Siebold, C. & Rohatgi, R. Biochemical mechanisms of vertebrate hedgehog signaling. *Development* **146**, doi:10.1242/dev.166892 (2019).

38 Jeong, J., Mao, J., Tenzen, T., Kottmann, A. H. & McMahon, A. P. Hedgehog signaling in the neural crest cells regulates the patterning and growth of facial primordia. *Genes Dev* **18**, 937-951, doi:10.1101/gad.1190304 (2004).

39 Long, F., Zhang, X. M., Karp, S., Yang, Y. & McMahon, A. P. Genetic manipulation of hedgehog signaling in the endochondral skeleton reveals a direct role in the regulation of chondrocyte proliferation. *Development* **128**, 5099-5108 (2001).

40 Bastida, M. F. *et al.* The formation of the thumb requires direct modulation of Gli3 transcription by Hoxa13. *Proc Natl Acad Sci U S A* **117**, 1090-1096, doi:10.1073/pnas.1919470117 (2020).

41 Sanders, T. A., Llagostera, E. & Barna, M. Specialized filopodia direct long-range transport of SHH during vertebrate tissue patterning. *Nature* **497**, 628-632, doi:10.1038/nature12157 (2013).

42 Alon, U. *An introduction to systems biology : design principles of biological circuits*. (Chapman & Hall/CRC, 2007).

43 Lex, R. K. *et al.* GLI transcriptional repression regulates tissue-specific enhancer activity in response to Hedgehog signaling. *Elife* **9**, e50670, doi:10.7554/eLife.50670 (2020).

44 Hasson, P., Del Buono, J. & Logan, M. P. Tbx5 is dispensable for forelimb outgrowth. *Development* **134**, 85-92, doi:10.1242/dev.02622 (2007).

45 Xu, X. *et al.* Fibroblast growth factor receptor 2 (FGFR2)-mediated reciprocal regulation loop between FGF8 and FGF10 is essential for limb induction. *Development* **125**, 753-765 (1998).

46 Dahn, R. D. & Fallon, J. F. Interdigital regulation of digit identity and homeotic transformation by modulated BMP signaling. *Science* **289**, 438-441, doi:10.1126/science.289.5478.438 (2000).

47 Suzuki, T., Hasso, S. M. & Fallon, J. F. Unique SMAD1/5/8 activity at the phalanx-forming region determines digit identity. *Proc Natl Acad Sci U S A* **105**, 4185-4190, doi:10.1073/pnas.0707899105 (2008).

48 Witte, F., Chan, D., Economides, A. N., Mundlos, S. & Stricker, S. Receptor tyrosine kinase-like orphan receptor 2 (ROR2) and Indian hedgehog regulate digit outgrowth mediated by

the phalanx-forming region. *Proc Natl Acad Sci U S A* **107**, 14211-14216, doi:10.1073/pnas.1009314107 (2010).

49 Pickering, J. & Towers, M. Inhibition of Shh signalling in the chick wing gives insights into digit patterning and evolution. *Development* **143**, 3514-3521, doi:10.1242/dev.137398 (2016).

50 Gao, B. *et al.* A mutation in Ihh that causes digit abnormalities alters its signalling capacity and range. *Nature* **458**, 1196-1200, doi:10.1038/nature07862 (2009).

51 Pickering, J., Chinnaiya, K. & Towers, M. An autoregulatory cell cycle timer integrates growth and specification in chick wing digit development. *Elife* **8**, e47625, doi:10.7554/eLife.47625 (2019).

52 Li, D. Y. *et al.* Formation of Proximal and Anterior Limb Skeleton Requires Early Function of Irx3 and Irx5 and Is Negatively Regulated by Shh Signaling. *Developmental Cell* **29**, 233-240, doi:10.1016/j.devcel.2014.03.001 (2014).

53 Zhulyn, O. *et al.* A switch from low to high Shh activity regulates establishment of limb progenitors and signaling centers. *Dev Cell* **29**, 241-249, doi:10.1016/j.devcel.2014.03.002 (2014).

54 Lewis, P. M. *et al.* Cholesterol modification of sonic hedgehog is required for long-range signaling activity and effective modulation of signaling by Ptc1. *Cell* **105**, 599-612, doi:10.1016/s0092-8674(01)00369-5 (2001).

55 Chiang, C. *et al.* Cyclopia and defective axial patterning in mice lacking Sonic hedgehog gene function. *Nature* **383**, 407-413, doi:10.1038/383407a0 (1996).

56 Buscher, D., Grotewold, L. & Ruther, U. The XtJ allele generates a Gli3 fusion transcript. *Mamm Genome* **9**, 676-678, doi:10.1007/s003359900845 (1998).

57 Nguyen, M. T., Zhu, J., Nakamura, E., Bao, X. & Mackem, S. Tamoxifen-dependent, inducible Hoxb6CreERT recombinase function in lateral plate and limb mesoderm, CNS isthmic organizer, posterior trunk neural crest, hindgut, and tailbud. *Dev Dyn* **238**, 467-474, doi:10.1002/dvdy.21846 (2009).

58 Soriano, P. Generalized lacZ expression with the ROSA26 Cre reporter strain. *Nat Genet* **21**, 70-71, doi:Doi 10.1038/5007 (1999).

59 Srinivas, S. *et al.* Cre reporter strains produced by targeted insertion of EYFP and ECFP into the ROSA26 locus. *BMC developmental biology* **1**, 4 (2001).

60 Logan, M. *et al.* Expression of Cre Recombinase in the developing mouse limb bud driven by a Prx1 enhancer. *Genesis* **33**, 77-80, doi:10.1002/gene.10092 (2002).

61 Nakamura, E., Nguyen, M. T. & Mackem, S. Kinetics of tamoxifen-regulated Cre activity in mice using a cartilage-specific CreER(T) to assay temporal activity windows along the proximodistal limb skeleton. *Dev Dyn* **235**, 2603-2612, doi:10.1002/dvdy.20892 (2006).

62 Wilkinson, D. Whole mount in situ hybridization of vertebrate embryos. In In Situ Hybridization: A practical Approach, D. G. Wilkinson, ed. (Oxford: IRL Press), pp. 75-83. (1992).

63 Kessel, M. & Gruss, P. Homeotic transformations of murine vertebrae and concomitant alteration of Hox codes induced by retinoic acid. *Cell* **67**, 89-104, doi:10.1016/0092-8674(91)90574-i (1991).

Figure legends:

Figure 1. A transient pulse of Shh activity is both necessary and sufficient to specify all digits if cell survival is enforced.

a, Diagram of Shh expression timeline in wildtype mouse hindlimb buds at successive embryo stages, with Shh/ZPA in green. Axis orientation for early limb buds, digit condensation (E12.5) and late skeletal (E16.5) stages indicated at left. Hindlimb Shh expression initiates at E10 and ceases around E12 (~48 hrs). Duration of patterning by Shh (~2-3 hrs) compared to cell survival/expansion role in outgrowth (48 hrs) summarized from results in **b,c** below.

b, Assay of Shh activity (direct response) by *Ptch1* RNA expression after tamoxifen treatment (at times post-treatment indicated by timeline) in control (*Shh*$^{+/c}$;*Bax*-CKO, upper panels) and in *Shh*-CKO;*Bax*-CKO hindlimb buds (lower panels). Note that Shh expression initiates at about 6-8 hrs after the time of tamoxifen injection (a). No activity was detected in either control (n=9) or *Shh*-CKO;*Bax*-CKO hindlimbs at 4h after tamoxifen dosage (n=7). Shh activity was first detected at 6h after tamoxifen injection in a subset of control (7/12, arrow) and in *Shh*-CKO;*Bax*-CKO (7/15, arrow) embryos, and became consistent and robust by 8hr in control (n=12, arrow), but was absent in all *Shh*-CKO;*Bax*-CKO embryos (n=10). Limb buds in all panels oriented with anterior at top and distal at right. so, somite.

c, Skeletal staining (E16.5) following *Bax/Bak* and *Shh* removal by tamoxifen (given at E9.5+3h, as in **b**). In control hindlimbs with *Bax/Bak* function present (Bax [+], *Bax*$^{+/c}$; upper panels) all *Shh*-CKO embryos (28/28) have a single digit structure with phenotype the same as *Shh* null (*Shh*$^{-/-}$). In hindlimbs with *Bax/Bak* function absent (Bax [-], *Bax*$^{c/c}$; lower panels), about half of the *Shh*-CKO embryos (18/31) have between 3-5 normal digits and normal zeugopod elements (tibia, fibula), but all *Shh* null embryos (*Shh*$^{-/-}$, n=18/18) with *Bax/Bak* removal retain the null mutant phenotype . Right most panel shows an example of *Shh*-CKO;*Bax*-CKO with 5-digit phenotype. All limb skeletons oriented with anterior (digit 1) at left and distal at top of panel. Ti: tibia; Fi: fibula.

Figure 2. Rescued digit formation in *Shh*-CKO;*Bax*-CKO embryos is not due to pathway re-activation, but expression of targets implicated in outgrowth and patterning is maintained.

a, RNA expression of genes monitoring Shh pathway activity (*Hand2, Ptch1*) and Shh targets that

regulating outgrowth/patterning (*Grem1, Hoxa13, Hoxd13*) at E10.5-10.75 and at E11.5, after *Shh* removal by tamoxifen at E9.5+3h (as in Fig. 1b). *Bax/Bak* function absent (*Bax*-CKO) in all embryo genotypes. No *Hand2* or *Ptch1* is detected in *Shh*-CKO;*Bax*-CKO hindlimb buds or in *Shh* null ($Shh^{-/-}$;*Bax*-CKO). *Grem1* and *Hoxa13* expression at both E10.75 and E11.5, and *Hoxd13* late phase distal expression at E11.5 are sustained in a subset (about 50%) of *Shh*-CKO;*Bax*-CKO hindlimbs, in contrast to $Shh^{-/-}$; *Bax*-CKO. Mutant numbers analyzed giving the result shown are indicated in each panel. In remaining *Shh*-CKO;*Bax*-CKO embryos, expression is unchanged from $Shh^{-/-}$; *Bax*-CKO (absent, markedly reduced). All limb buds oriented with anterior at top and distal at right.

b, Immunofluorescence quantitation of Gli3 full-length (Gli3 FL) and repressor (Gli3 R) protein at E10.5, following *Bax/Bak* and *Shh* removal as in Fig 1b. Typical blot shown to left with anti-Gli3 (green) and anti-vinculin (red) shows elevated Gli3R in *Shh*-CKO;*Bax*-CKO and $Shh^{-/-}$;*Bax*-CKO compared to control ($Shh^{+/-}$;*Bax*-CKO). Immunofluorescence quantification of Gli3 FL/R ratio shown to right in bar-graph; N indicates numbers of independent samples (single hindlimb pairs) analyzed for each genotype. Gli3 FL/R is equivalently reduced in *Shh*-CKO;*Bax*-CKO (p=0.00002) and in $Shh^{-/-}$;*Bax*-CKO (p=0.001) compared to control hindlimb buds , and Gli3 FL/R shows no significant difference between *Shh*-CKO;*Bax*-CKO and $Shh^{-/-}$;*Bax*-CKO (p=0.48). ***, p <0.001.

c, Effect of *Gli3* dosage reduction ($Gli3^{+/-}$) on *Shh*-CKO and $Shh^{-/-}$ skeletal phenotypes (E16.5). Unlike *Bax/Bak* removal (*Bax*-CKO), *Gli3* dosage reduction alone results in a *Shh*-CKO phenotype that is unchanged from $Shh^{-/-}$;$Gli3^{+/-}$, and fails to restore normal limb morphology (arrow bar). Further removal of *Bax/Bak* in $Shh^{-/-}$;$Gli3^{+/-}$ (center panel) did not change the skeletal phenotype from $Shh^{-/-}$;$Gli3^{+/-}$. Numbers analyzed with the phenotype shown are indicated at bottom of each panel. All limb skeletons oriented with anterior (digit 1, tibia) at left and distal at top of panel.

Figure 3. Lineage tracing of *Shh* expression and response in wild-type embryos at time of *Shh* expression onset.

a, Distribution of RosaLacZ reporter+ descendant cells after a single Tamoxifen dose injected at stages indicated. Embryos were collected several days later at E13.5 to visualize hindlimb digit rays and identify contribution of descendants to each digit (data summarized in **b**). Both $Shh^{CreER/+}$ and $Gli1^{CreER/+}$ alleles were present in single crosses to enable comparison of descendants from *Shh*-expressing ($Shh^{CreER/+}$;$Rosa^{LacZ/LacZ}$, top row) and Shh-responding ($Gli1^{CreER/+}$;$Rosa^{LacZ/LacZ}$,

bottom row) cells in sibling embryos (positive for a single Cre allele) under identical conditions (embryo age, tamoxifen dose). Tamoxifen treatment at E9.5 or E9.75 (time window when transient Shh activity restores normal limb development in *Shh*-CKO;*Bax*-CKO) shows that direct Shh-response is limited to the digit 4, 5 territory. Long-range response in digit 2-3 territory becomes prominent later, by E10.5. All limb buds oriented with anterior (digit 1) at left and distal at top of panel.

b, Summary diagram of data in (**a**) shows tamoxifen activity time window (red bar) overlap with *Shh* expression/response (solid/hatched green in hindlimb outlines) and the digit contributions of ZPA or Shh-responsive descendants (to right) for each tamoxifen injection time analyzed in (**a**). Effective tamoxifen duration was estimated to be about 12 hours (from ref[78] and data in Figs 1b, extended data Figure 1a). Tamoxifen injected at 12 hours (E9.5) or 6 hours (at E9.75) before *Shh* expression onset (at ~ E10 in hindlimbs) result in narrow CreER activity duration times (short red bars in top 2 rows), that label an early population of *Shh*-expressing (ZPA; panel **a**-top row) and direct responding (panel **a**-bottom row) cells during the Shh activity time window necessary and sufficient for normal digit specification (Fig. 1). These early responding cells only contribute to d4 and d5 (hatched green in the left diagram of E13.5 hindlimb), indicating d2 and d3 are specified by indirect mechanism (blue). Cells respond to late Shh, important for cell survival/growth, contribute to d2 – d5 (hatched green in the right diagram of E13.5 hindlimb).

Figure 4. Relay signals downstream of enforced Hh-response in ZPA domain restore normal digit 1 formation in *Shh*$^{-/-}$ null limbs.

a, Schematic of strategy to detect relay signals from ZPA. *Shh*^{Cre} knock-in (KI), mutant allele crossed with *Shh*$^{+/-}$;*Rosa*^{SmoM2} activates Shh-response in the ZPA of *Shh* null limb bud (*Shh*$^{cre/-}$) cell-autonomously. Phenotypic changes in non-ZPA digits would require a non-autonomous downstream signal (relay).

b, Skeletal phenotypes (E16.5) of *Shh* null limbs with enforced Shh-response (SmoM2 active in ZPA domain). A normal digit 1 (d1) is restored in both forelimbs and hindlimbs in *Shh*$^{cre/-}$;Shh-SmoM2+ embryos with high efficiency (21/32; right panels). Note that posterior digits (4, 5) are dysmorphic and uninterpretable due to constitutive Hedgehog pathway activation during chondrogenic differentiation (see also Extended data Figure 3). Limbs oriented with anterior at

left and distal at top of panel.

c, LacZ reporter expression in ZPA-derived lineage in E11.5 and E14.5 hindlimbs. At E14.5, although ZPA descendants extend anteriorly in *Shh*$^{cre/-}$;Shh-SmoM2+(middle panels), the anterior-most digit is devoid of LacZ+ cells (5/5, arrow). In contrast, the single dysmorphic digit in *Shh* null (*Shh*$^{Cre/-}$; left panels) arises entirely from LacZ+ ZPA descendant cells (7/7). Close-up of footplate skeletal phenotypes (E16.5) shown in bottom row for comparison. In all panels, limb buds and limbs are oriented with anterior (digit 1) at left and distal at top of panel.

d, *Hoxa13* RNA expression at E11.5 in distal limb buds is restored in *Shh*$^{cre/-}$;Shh-SmoM2+ (6/6; middle panel, forelimb shown), but is absent in *Shh* null (*Shh*$^{Cre/-}$; left panel forelimb). All limb buds are oriented with anterior at top and distal at right of panel.

e, Model for digit specification by early Shh activity. Shh is required transiently to specify non-ZPA digits (d1-d3), including digit 1 (d1), by activating relay signals in the ZPA domain. Prior work has shown that direct Shh signaling uniquely inhibits d1 specification[52,53]. Together, direct repression and indirect promotion establish a unique regulatory network for d1 (thumb). Unlike d1-d3, ZPA-descended digits (d4, d5) do respond directly to Shh signaling early, but whether this direct signaling is essential, or if relay signals also play a role in d4,d5 specification has not been excluded in this study. We propose that the relay signaling initiated by early transient Shh activity plays a role in establishing late graded interdigit signaling centers that ultimately regulate final digit identity. Continued late Shh activity is required for sustained cell survival during expansion of limb bud digit progenitors.

Extended Data Figure legends:

Extended Data Figure 1. Duration of Shh activity and enforced cell survival in *Shh*-CKO;*Bax*-CKO embryos.

a, Assay of Shh activity (direct response) by *Gli1* RNA expression after tamoxifen treatment (at times post-treatment indicated by timeline) in control (*Shh*$^{+/c}$;*Bax*-CKO, upper panels) and in *Shh*-CKO;*Bax*-CKO hindlimb buds (lower panels). Note that Shh expression initiates at about 6-8 hrs after the time of tamoxifen injection. No activity is detected in either control (n=10) or *Shh*-CKO;*Bax*-CKO (n=9) hindlimbs at 3h after tamoxifen dosage. Shh activity was first detected at 6h

after tamoxifen injection in a subset of control (6/10, arrow) and *Shh*-CKO;*Bax*-CKO (4/10, arrow) hindlimb buds, and became consistent and strong by 9h in control (n=9), but was absent in all *Shh*-CKO;*Bax*-CKO embryos (n=11). Limb buds in all panels oriented with anterior at top and distal at right. so, somite.

b, Lysotracker staining for cell death at E10.75, following *Bax/Bak* and *Shh* removal with tamoxifen at E9.5+3h (as in panel **a**). In control hindlimbs with *Bax/Bak* function present (Bax [+], $Bax^{+/c}$; upper panels) all *Shh*-CKO embryos (10/10) have extensive apoptosis at the same level as *Shh* null mutant ($Shh^{-/-}$, n=7). In hindlimbs with *Bax/Bak* function deleted (Bax [-], $Bax^{c/c}$; lower panels), no apoptosis is detected in either *Shh*-CKO (11/11) or in $Shh^{-/-}$ null (9/9) hindlimb buds. Note that *Hoxb6CreER* is not expressed in somites, where apoptosis remains present. Limb buds in all panels oriented with anterior at top and distal at right.

Extended Data Figure 2. Expression of Shh target genes implicated in limb bud outgrowth and digit patterning, but not in Shh-pathway activity, is maintained in *Shh*-CKO;*Bax*-CKO.

No expression of *Gli1* is detected in *Shh*-CKO;*Bax*-CKO hindlimb buds or in *Shh* null ($Shh^{-/-}$;*Bax*-CKO) at E11.5, indicating a lack of Shh pathway reactivation. In contrast, *Fgf8*, *Jag1*, *Cyp26b1*, and *Hoxd11* expression at E10.75 and E11.5 are sustained in a subset (about 50%) of *Shh*-CKO;*Bax*-CKO hindlimbs. In $Shh^{-/-}$;*Bax*-CKO, *Cyp26b1* and *Hoxd11* expression were preserved at E10.75, but markedly reduced or lost by E11.5; *Fgf8* was still expressed, but at a reduced level by E11.5. *Fgf8* was only evaluated at E11.5 because expression is unaltered even in $Shh^{-/-}$ null at E10.75[11]. Mutant numbers analyzed with the result shown are indicated in each panel. In remaining *Shh*-CKO;*Bax*-CKO embryos, expression was unchanged from $Shh^{-/-}$;*Bax*-CKO. The lower set of panels show *Hoxd13* expression at E12.5, which is maintained in *Shh*-CKO;*Bax*-CKO with phenotypic rescue of footplate (4/4), and in the digit rudiment of litter mate *Shh*-CKO;$Bax^{+/-}$ hindlimbs (2/2) similarly to the $Shh^{-/-}$;*Bax*-CKO. All limb buds oriented with anterior at top and distal at right.

Extended Data Figure 3. A bona fide digit 1 is restored in $Shh^{cre/-}$;Shh-SmoM2+ limbs and is not a consequence of cryptic anterior Hedgehog ligand/pathway activation.

a, Skeletal staining (E17.5) and ZPA lineage tracing (E14.5) of control $Shh^{cre/+}$;Shh-SmoM2 (*Shh*+)

embryos. In control *Shh*$^{cre/+}$;Shh-SmoM2+, posterior digits are dysmporphic and uninterpretable because of constitutive Hedgehog pathway activation (brackets in middle 2 panels), and a small percentage of limbs have preaxial polydactyly (*, 4/64), related to ectopic anterior Shh activation revealed by ZPA lineage tracing at E14.5 (LacZ+, arrow). The single digit in *Shh* null arises entirely from ZPA descendants (right panels). Ti: tibia; Fi: fibula. Limb skeletons (and **b** panels) oriented with anterior (digit 1, tibia) at left and distal at top of panel.

b, *Uncx4.1* RNA expression in E14.5 forelimbs. *Uncx4.1* is expressed exclusively in digit 1 in control forelimbs (*Shh*$^{+/-}$; left panel), and is expressed in the rescued digit 1 in *Shh*$^{cre/-}$;Shh-SmoM2+ (6/8; middle panel, arrow), but is not detected in *Shh*$^{-/-}$ limbs (n=4; right panel).

For (**c**) - (**d**), all limb buds are oriented with anterior at top and distal at right of panel.

c, *Ptch1* and *Gli1* RNA expression in E11.5 forelimbs. *Ptch1* and *Gli1* are expressed in the posterior limb buds in *Shh*$^{cre/-}$;Shh-SmoM2+, consistent with cell-autonomous Shh pathway activation in ZPA domain, but no expression is detected in the anterior limb bud (n=10, Ptch1; and n=8, Gli1).

d, Lysotracker staining (for cell death) and LacZ+ (or EYFP+) detection of ZPA lineage in *Shh*$^{cre/-}$;Shh-SmoM2+ limb buds. Apoptosis persists in anterior non-ZPA descended limb bud in *Shh*$^{cre/-}$;Shh-SmoM2+ limb buds similar to *Shh* null (*Shh*$^{-/-}$) at E10.75 and E11.5, but subsides by E12.5. *Rosa*^{LacZ} or *Rosa*^{EYFP} Cre-reporters were used to mark ZPA lineage.

Table 1. list of genetic crosses, embryo numbers analyzed, and outcomes for experiments related to each figure.

Alleles crossed:	Shorthand notation:	% Rescued†	Tam Tx time:	phenotype/analysis:	related to Figure:
Shh$^{+/C}$;*Bax*$^{+/C}$;*Bak*$^{-/-}$;*Hoxb6CreER* x *Shh*$^{C/C}$;*Bax* $^{C/C}$;*Bak*$^{-/-}$;*Hoxb6CreER*	Shh-CKO;Bax-CKO Shh-CKO;Bax$^{+/c}$	18/31 (Bax-hom); 0/28 (Bax-het)	E9.5+3h	Limb skeleton	Fig. 1
Shh$^{+/-}$;*Bax*$^{+/C}$;*Bak*$^{-/-}$;*Hoxb6CreER*-hom x *Shh*$^{+/-}$;*Bax* $^{C/C}$;*Bak*$^{-/-}$	Shh$^{-/-}$;Bax-CKO	0/18 (Bax-hom)	E8.75-E9.5	limb skeleton	Fig. 1
Shh$^{+/-}$;*Bax* $^{+/-}$;*Bak*$^{-/-}$ x *Shh*$^{+/-}$;*Bax* $^{+/-}$;*Bak*$^{-/-}$	Shh$^{-/-}$;Bax$^{-/-}$	0/6 (relative to Shh-CKO;Bax-CKO)	NA	limb skeleton	Same as Fig.1
Shh$^{+/C}$;*Bax*$^{C/C}$;*Bak*$^{-/-}$;*Hoxb6CreER* x *Shh*$^{C/C}$;*Bax* $^{C/C}$;*Bak*$^{-/-}$;*Hoxb6CreER*	Shh-CKO;Bax-CKO	NA-see Fig. 1, ED1*, text	E9.5+3h	transient Shh activity detection	Fig. 1,ED1
Shh$^{+/-}$;*Bax*$^{+/C}$;*Bak*$^{-/-}$;*Hoxb6CreER*-hom x *Shh*$^{-/C}$;*Bax* $^{C/C}$;*Bak*$^{-/-}$;*Hoxb6CreER*	Shh-CKO;Bax-CKO Shh$^{-/-}$;Bax-CKO	NA-see Fig. ED1, text	E9.5+3h	Cell survival	Fig. ED1
Shh$^{+/-}$;*Bax*$^{C/C}$;*Bak*$^{-/-}$;*Hoxb6CreER*-hom x *Shh*$^{-/C}$;*Bax* $^{C/C}$;*Bak*$^{-/-}$;*Hoxb6CreER*	Shh-CKO;Bax-CKO Shh$^{-/-}$;Bax-CKO	NA-see Fig. 2, ED2, text	E9.5+3h	Hh activity reporters: Hand2, Ptch1, Gli1 Gli3 western	Fig. 2,ED2
Shh$^{+/-}$;*Gli3*$^{+/-}$;*Bax*$^{C/C}$;*Bak*$^{-/-}$;*Hoxb6CreER*-hom x *Shh*$^{+/-}$;*Bax* $^{C/C}$;*Bak*$^{-/-}$;*Hoxb6CreER*	Shh$^{-/-}$;Gli3$^{+/-}$;BaxCKO	10/10 (relative to Shh$^{-/-}$)		limb skeleton - Gli3 dosage modulation	
Shh$^{+/-}$;*Gli3*$^{+/-}$ x *Shh*$^{C/C}$;*Hoxb6CreER*	Shh$^{-/-}$;Gli3$^{+/-}$ Shh-CKO;Gli3$^{+/-}$	8/8 (relative to Shh$^{-/-}$) 12/12 (relative to Shh-CKO)			
Shh$^{+/-}$;*Bax*$^{C/C}$;*Bak*$^{-/-}$;*Hoxb6CreER*-hom x *Shh*$^{-/C}$;*Bax* $^{C/C}$;*Bak*$^{-/-}$;*Hoxb6CreER*	Shh-CKO;Bax-CKO	18/31 (relative to Shh-CKO)	E9.5+3h or no tam		Fig. 2
Shh$^{+/-}$;*Bax*$^{C/C}$;*Bak*$^{-/-}$;*Hoxb6CreER*-hom x *Shh*$^{-/C}$;*Bax* $^{C/C}$;*Bak*$^{-/-}$;*Hoxb6CreER*	Shh-CKO;Bax-CKO Shh$^{-/-}$;Bax-CKO	NA-see Fig. 2, text	E9.5+3h	Shh target gene expression: Grem1, Hoxa13, Hoxd13	Fig. 2
Shh$^{+/-}$;*Bax*$^{C/C}$;*Bak*$^{-/-}$;*Hoxb6CreER*-hom x *Shh*$^{-/C}$;*Bax* $^{C/C}$;*Bak*$^{-/-}$;*Hoxb6CreER*	Shh-CKO;Bax-CKO Shh$^{-/-}$;Bax-CKO	NA-see Fig. ED2, text	E9.5+3h	Shh target gene expression: Jag1, Fgf8, Cyp26b1,Hoxd11, Hoxd13	Fig. ED2
Shh$^{CreER/+}$;*Rosa*$^{LacZ/LacZ}$ x *Gli1*$^{CreER/+}$;*Rosa*$^{LacZ/LacZ}$	ShhCreER+ or Gli1CreER+	-51 embryos analyzed -60 embryos analyzed NA-see Fig. 3, text	Various-see Fig 4	Shh-expressing (ZPA) and Shh-responding lineages	Fig. 3
Shh$^{Cre/+}$;*Rosa*$^{LacZ/LacZ}$ x *Shh*$^{+/-}$;*Rosa*$^{SmoM2/SmoM2}$ *Shh*$^{Cre/+}$;*Rosa*$^{LacZ/LacZ}$ x *Shh*$^{+/-}$	Shh$^{Cre/-}$;Shh-SmoM2 Shh$^{Cre/-}$	21/32 (digit 1+) 0/6 (digit 1+) NA-see Fig. 4, text	NA	Limb skeleton ZPA (LacZ) lineage, Hoxa13	Fig. 4
Shh$^{Cre/+}$;*Bax*$^{+/-}$;*Bak*$^{-/-}$;*Rosa*$^{LacZ/LacZ}$ x *Shh*$^{+/-}$;*Bax* $^{+/-}$;*Bak*$^{-/-}$;*Rosa*$^{SmoM2/+}$	Shh$^{Cre/-}$;Bax/Bak-KO; Shh-SmoM2	8/8 (only digit 1 restored)	NA	Limb skeleton	Same as Fig. 4
Shh$^{Cre/+}$;*Rosa*$^{LacZ/LacZ}$ x *Shh*$^{+/-}$;*Rosa*$^{SmoM2/+}$	Shh$^{Cre/+}$;Shh-SmoM2 Shh$^{Cre/-}$;Shh-SmoM2 Shh$^{Cre/-}$	4/64 (ectopic ZPA, extra duplicated anterior digit) NA-see Fig. ED3, text	NA	Limb skeleton ZPA (LacZ) lineage digit 1 marker: Uncx4.1 Hh activity: Ptch1, Gli1	Fig. ED3
Shh$^{Cre/+}$;*Rosa*$^{LacZ/LacZ}$ x *Shh*$^{+/-}$;*Rosa*$^{SmoM2/+}$ *Shh*$^{Cre/+}$;*Rosa*$^{EYFP/EYFP}$ x *Shh*$^{+/-}$;*Rosa*$^{SmoM2/+}$	Shh$^{Cre/-}$;Shh-SmoM2 Shh$^{Cre/-}$	-10 embryos analyzed - 6 embryos analyzed NA-see Fig. ED3, text	NA	ZPA (LacZ, EYFP) lineage; cell survival analysis	Fig. ED3

†skeletal numbers refer to embryo numbers (left+right hindlimb both rescued)

*ED, extended data figure

Figure 1.

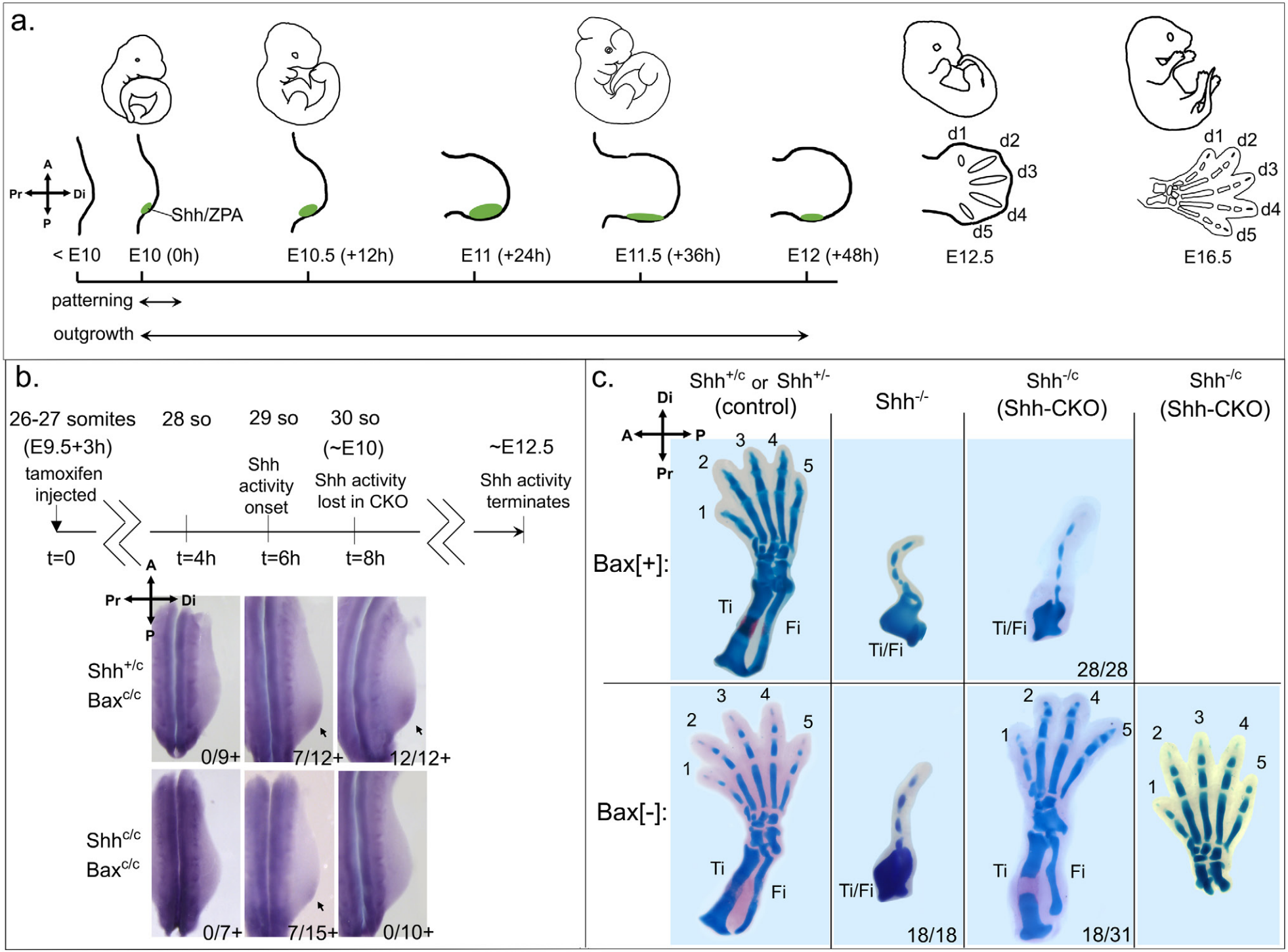
a.
A
Pr
Di
P
Shh/ZPA
< E10
E10 (0h)
E10.5 (+12h)
E11 (+24h)
E11.5 (+36h)
E12 (+48h)
d1
d2
d3
d4
d5
E12.5
E16.5
patterning
outgrowth
b.
26-27 somites
(E9.5+3h)
tamoxifen
injected
28 so
29 so
Shh
activity
onset
30 so
(~E10)
Shh activity
lost in CKO
~E12.5
Shh activity
terminates
t=0
t=4h
t=6h
t=8h
Shh+/c
Bax c/c
0/9+
7/12+
12/12+
Shhc/c
Bax c/c
0/7+
7/15+
0/10+
c.
Shh+/c or Shh+/-
(control)
Shh-/-
Shh-/c
(Shh-CKO)
Shh-/c
(Shh-CKO)
Bax[+]:
Bax[-]:
Ti
Fi
Ti/Fi
28/28
18/18
18/31

Figure 2.

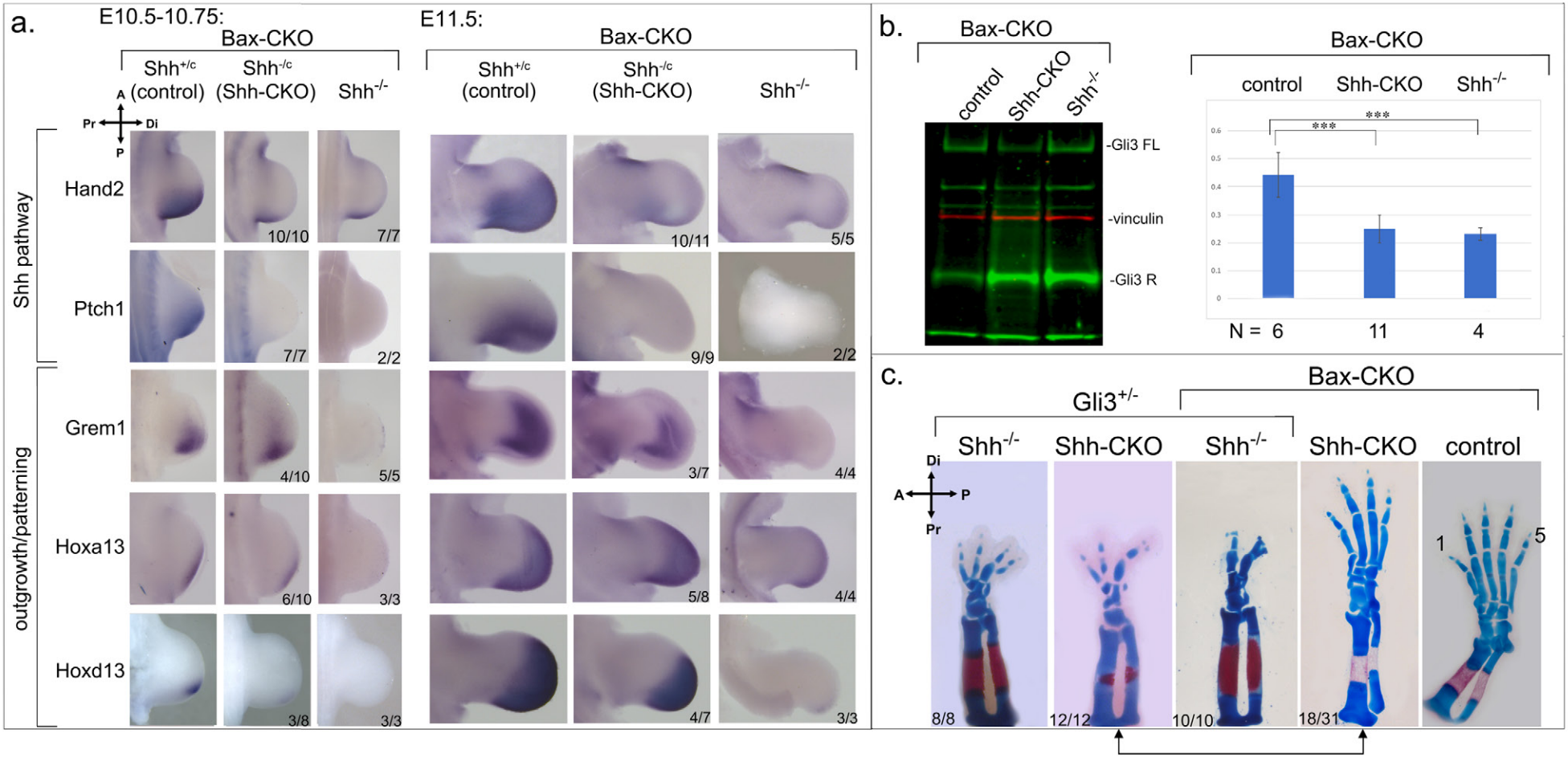
a.
E10.5-10.75:
Bax-CKO
Shh+/c (control)
Shh-/c (Shh-CKO)
Shh-/-
E11.5:
Bax-CKO
Shh+/c (control)
Shh-/c (Shh-CKO)
Shh-/-
A
P
Pr
Di
Shh pathway
outgrowth/patterning
Hand2
Ptch1
Grem1
Hoxa13
Hoxd13
10/10
7/7
7/7
2/2
10/11
5/5
9/9
2/2
4/10
5/5
3/7
4/4
6/10
3/3
5/8
4/4
3/8
3/3
4/7
3/3
b.
Bax-CKO
control
Shh-CKO
Shh-/-
-Gli3 FL
-vinculin
-Gli3 R
Bax-CKO
control
Shh-CKO
Shh-/-
***
***
N = 6
11
4
c.
Gli3+/-
Bax-CKO
Shh-/-
Shh-CKO
Shh-/-
Shh-CKO
control
Di
A
P
Pr
8/8
12/12
10/10
18/31
1
5

Figure 3.

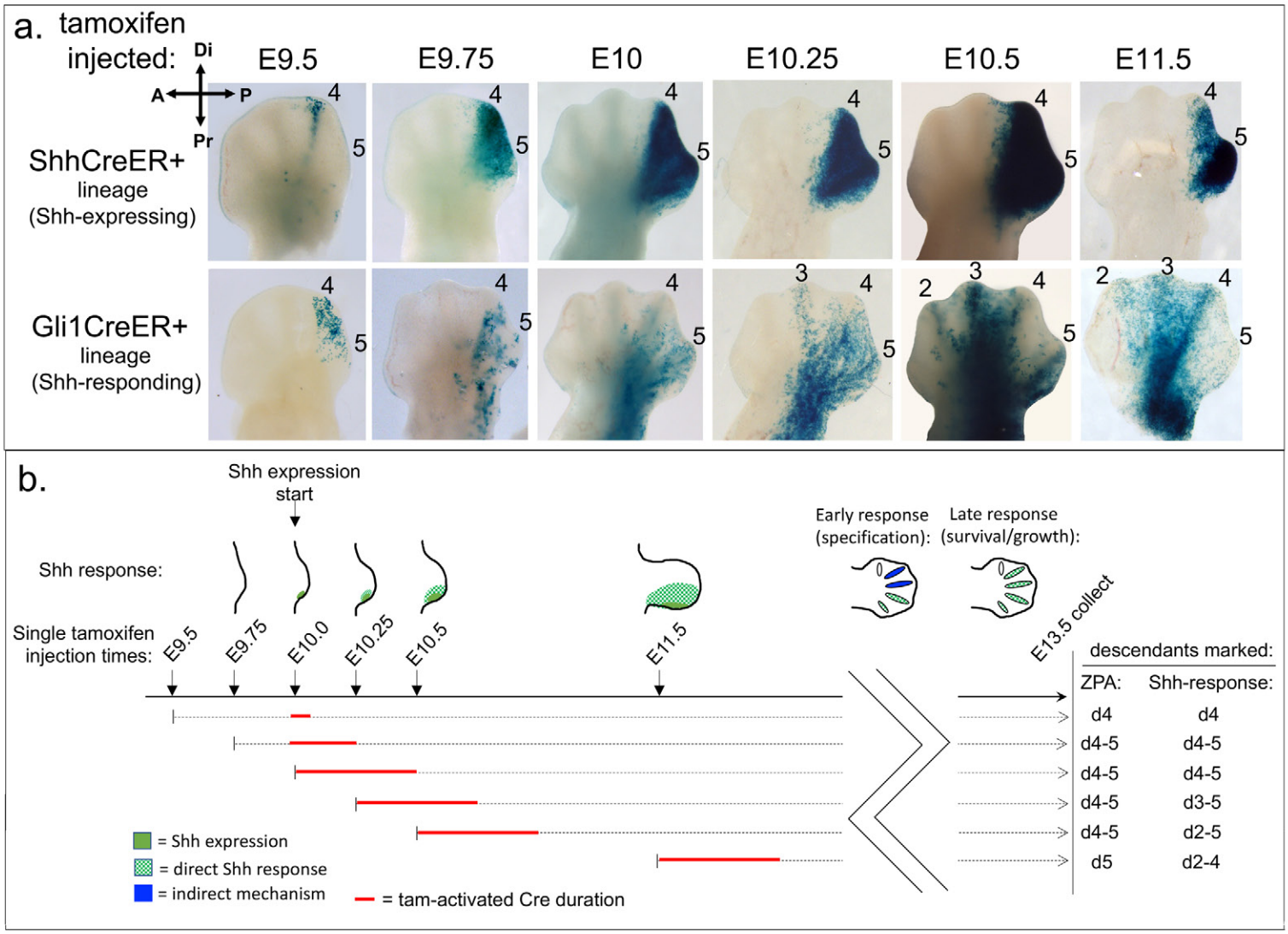

Figure 4.

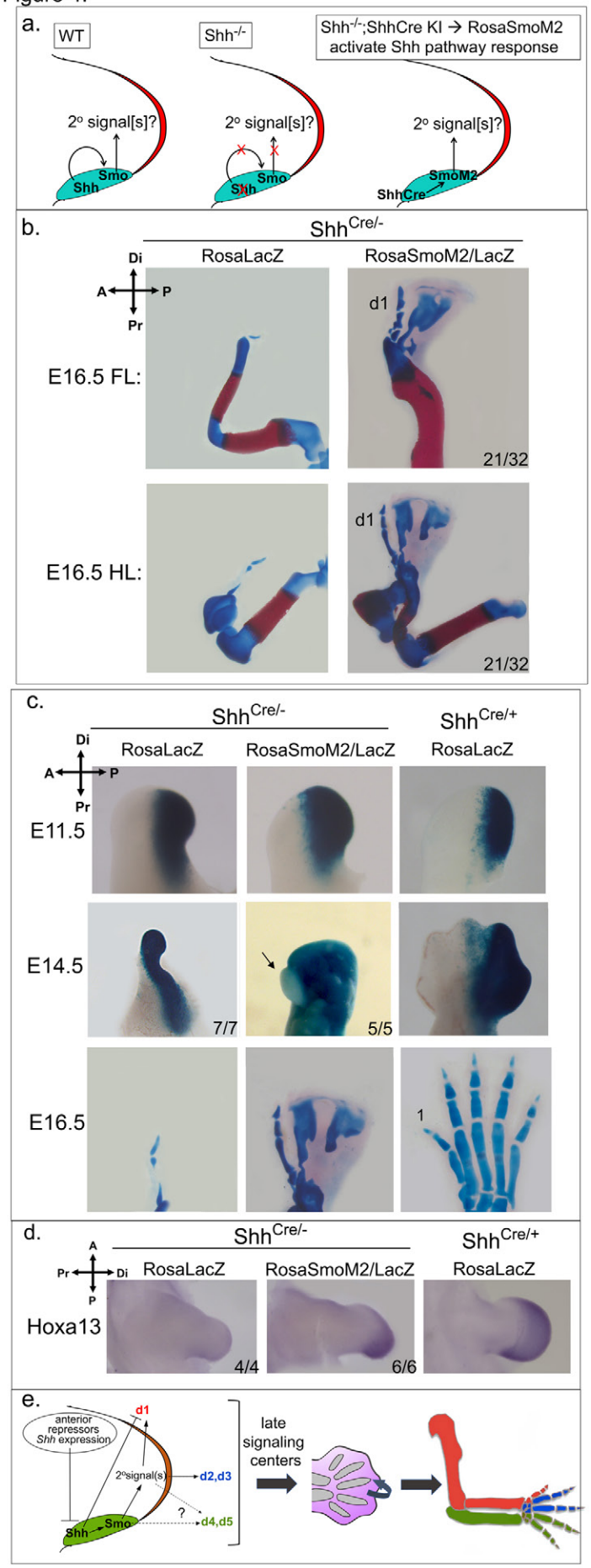

Extended data Figure 1:

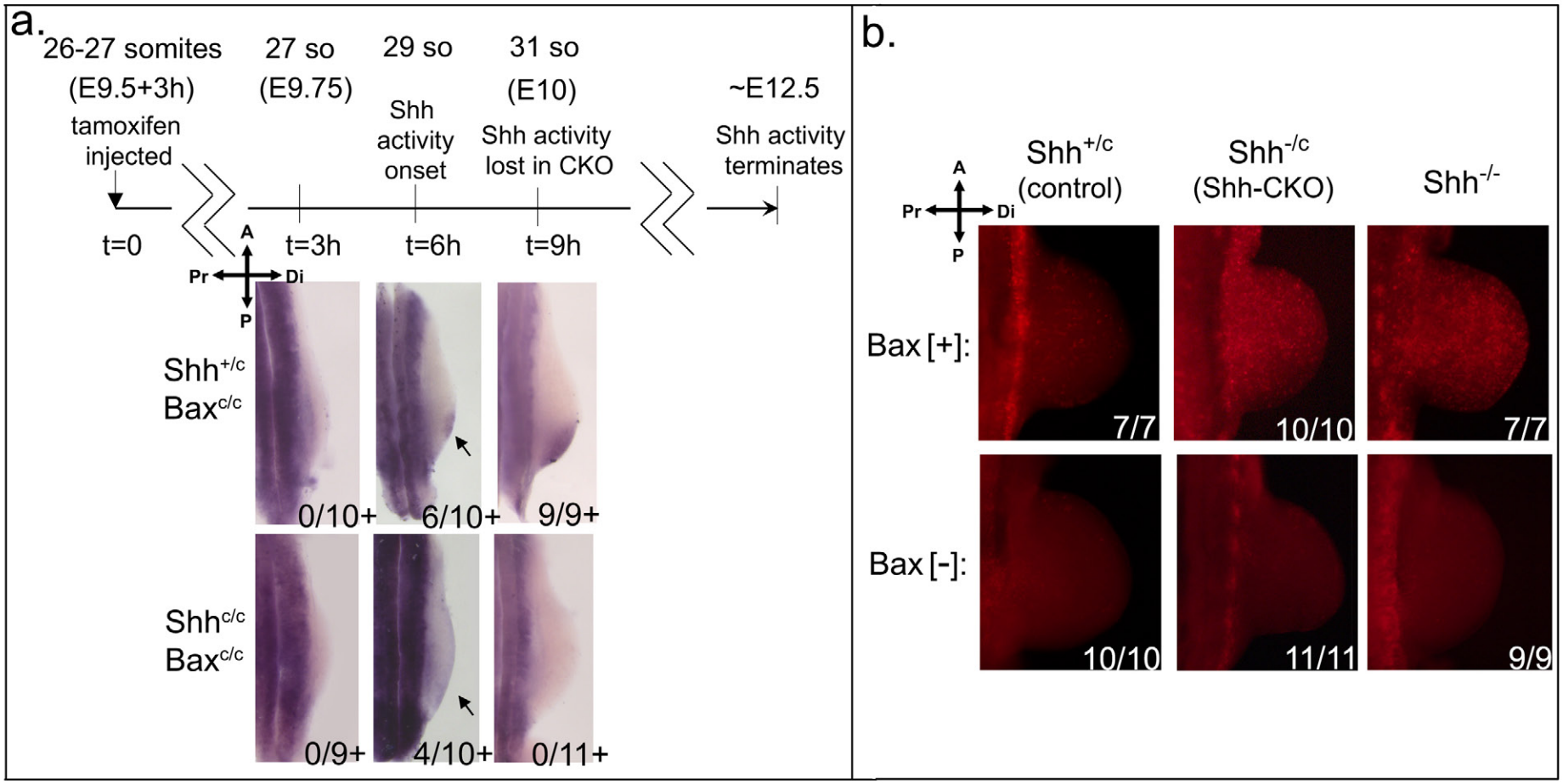

Extended Data Figure 2:

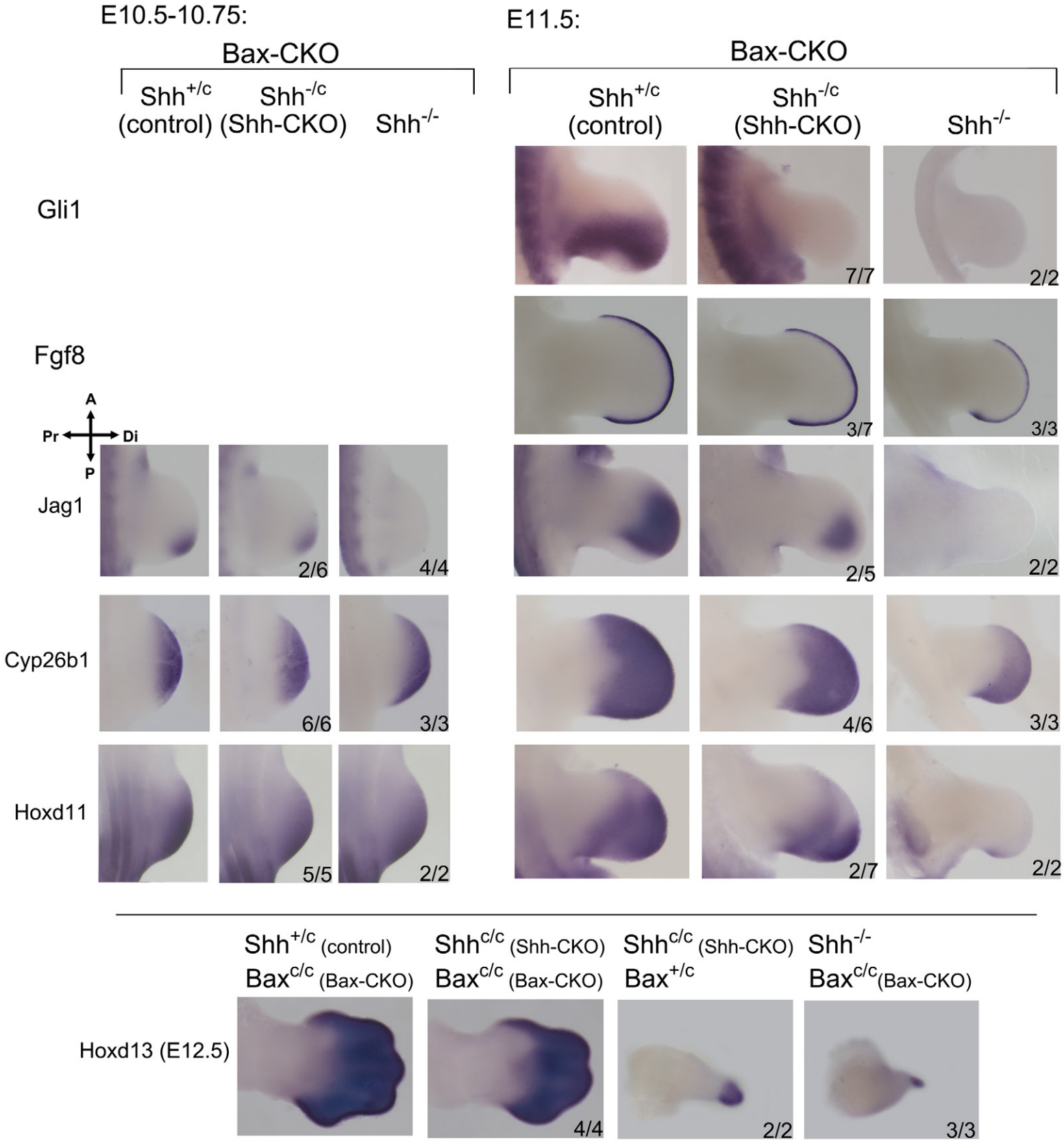

Extended Data Figure 3: